NASA TECHNICAL NOTE

NASA TN D-2957

NASA TN D-2957

INFLUENCE OF COMBUSTION PROCESS ON STABILITY

by Richard J. Priem

Lewis Research Center
Cleveland, Ohio

NATIONAL AERONAUTICS AND SPACE ADMINISTRATION • WASHINGTON, D. C. • AUGUST 1965

NASA TN D-2957

INFLUENCE OF COMBUSTION PROCESS ON STABILITY

By Richard J. Priem

Lewis Research Center
Cleveland, Ohio

NATIONAL AERONAUTICS AND SPACE ADMINISTRATION

For sale by the Clearinghouse for Federal Scientific and Technical Information
Springfield, Virginia 22151 – Price $2.00

INFLUENCE OF COMBUSTION PROCESS ON STABILITY*

by Richard J. Priem

Lewis Research Center

SUMMARY

The relative importance of various steps in the combustion process on combustion instability was compared theoretically by assuming that individual steps controlled the growth of a disturbance. The combustion steps involved the time dependence of (1) propellant injection, (2) accumulation of unburned propellant, (3) propellant atomization, (4) propellant vaporization, and (5) chemical reaction. The calculation gave stability limits (minimum disturbance that will grow to instability) with various steps considered to control the combustion rate.

The calculations show that chemical reaction is the most sensitive mechanism, but if accumulation of unburned propellants is included, the chemical reaction step is likely to be important only for low conversion rates that do not occur in most rocket combustors. With realistic combustion conditions the physical processes of vaporization and atomization appear to be the most important in determining instability limits, the limits for each step depending on the accumulation of unburned propellant and vortex velocity. Experimental instability studies with an 8-foot torus combustor, which is similar in geometry to that used for the theoretical calculations, confirmed the calculated results. Experiments also confirmed qualitatively the fluctuations that occur during instability.

INTRODUCTION

Combustion of propellants in a liquid rocket combustion chamber involves the reaction of a reducing agent (fuel) and an oxidizing agent to produce reaction products with the liberation of heat. This seemingly simple statement of a reaction between the reducing and oxidizing agents can become very complicated when the mechanism or steps are considered that occur between the injection of liquid propellants and the time or position that the final products are formed. Occurring simultaneously with the combustion are fluctuations in the chamber pressure, which, under certain conditions, are seen to amplify into periodic oscillations driven by the combustion process. These periodic

*Presented at the 56th National Meeting of the A. I. Ch. E., San Francisco, Calif., May 16-19, 1965.

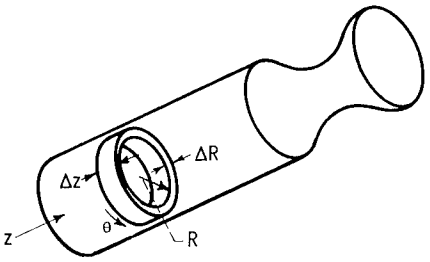

Figure 1. - Combustion section considered for various instability models.

pressure oscillations result in engine failure due to excessive heat transfer to the walls, which eventually leads to thermal failure, or vibrational interference with controls and other accessories that leads to mechanical failure. Thus, it is important to understand the role of the combustion process in the growth of these oscillations.

Previous studies have shown how various parts of the complicated combustion process could support the growth of a pressure disturbance. (See bibiography in ref. 1.) These studies have usually resulted in qualitative descriptions of the combustion process with pressure oscillations or a theory for a particular step that could sustain an oscillation. In each study the assumptions, combustor design, model, etc., are different; thus, it is impossible to evaluate the importance of a particular step in the combustion process in supporting the growth of a pressure disturbance. Therefore, a theoretical study was conducted, similar to that reported in reference 2 which used a toroidal ring to represent the combustor, in which the various combustion steps were individually assumed to control the growth of a disturbance. It was determined which step could amplify the smallest disturbance, so that this process could be further studied under more realistic and complicated conditions. To determine the influence of a vortex in the combustor, which may be produced by viscous forces with a transverse oscillation (ref. 3), calculations were also made with a constant vortex velocity superimposed on the oscillations. As a check on the theory, the calculated stability limits were compared to the experimental limits obtained with several injectors in a torus combustor.

THEORY

General Equations

The combustor geometry and transport equations used in the analytical portion of this investigation are identical to those in reference 2. The combustor was an annular section with a very small thickness ΔR and length Δz, as shown in figure 1. This geometry limits the oscillation to a transverse wave. The propellants are assumed to be uniformly injected and to burn at some rate which depends on their position within the combustor. The burning is accompanied by gas and liquid flow in the axial direction. As the propellants burn, random disturbances occur within the combustor. If the amplitude of a disturbance is large enough, it may develop into a wave in the combustor. The object of this study was to determine analytically, for various combustion steps, the

minimum amplitude of a pressure disturbance in the annulus that is needed to develop a wave. This calculation was accomplished by solving the transport equations that follow, which are derived in reference 2. Cylindrical coordinates are used in which the z-direction corresponds to the axial direction in the combustor.

Continuity

$$\frac{1}{2\pi}\frac{\partial \rho'}{\partial t'} + \rho'\left(\frac{\partial v_\theta'}{\partial \theta'} + \frac{\partial v_z'}{\partial z'}\right) + v_\theta'\frac{\partial \rho'}{\partial \theta'} + v_z'\frac{\partial \rho'}{\partial z'} = \mathscr{L}\omega' f(\gamma) \tag{1}$$

Momentum in θ-direction

$$\frac{\rho'}{2\pi}\frac{\partial v_\theta'}{\partial t'} + \rho' v_\theta'\frac{\partial v_\theta'}{\partial \theta'} + \frac{1}{\gamma}\frac{\partial P_c'}{\partial \theta'} + \mathscr{L}\omega' v_\theta' f(\gamma) = \frac{4}{3}\mathscr{J}\frac{\partial^2 v_\theta'}{(\partial \theta')^2} f(\gamma) \tag{2}$$

Energy

$$\frac{\rho'}{2\pi}\left(\frac{\partial T'}{\partial t'} + v_\theta'\rho'\frac{\partial T'}{\partial \theta'} + v_z'\rho'\frac{\partial T'}{\partial z'}\right) + (\gamma - 1)P_c'\left(\frac{\partial v_\theta'}{\partial \theta'} + \frac{\partial v_z'}{\partial z'}\right)$$

$$= \mathscr{J}\frac{\partial^2 T'}{(\partial \theta')^2} f(\gamma) + \mathscr{L}\omega'\left\{(\gamma - T') + \frac{\gamma - 1}{2}\gamma\left[(\Delta v')^2 + (v_\theta')^2\right]\right\} f(\gamma)$$

$$+ \frac{4}{3}\gamma(\gamma - 1)\mathscr{J}\left[\left(\frac{\partial v_\theta'}{\partial \theta'}\right)^2 + \left(\frac{\partial v_z'}{\partial z'}\right)^2 - \frac{\partial v_\theta'}{\partial \theta'}\frac{\partial v_z'}{\partial z'}\right] f(\gamma) \tag{3}$$

Ideal gas

$$\frac{\partial P_c'}{\partial \theta'} = T'\frac{\partial \rho'}{\partial \theta'} + \rho'\frac{\partial T'}{\partial \theta'} \tag{4}$$

(Symbols are defined in appendix A.) The derivatives in the axial (z) direction were determined with the assumption that the total mass, momentum, and energy in the annulus were constant. Furthermore, it was assumed that these derivatives were independent of θ. These assumptions result in the following equations (derived in ref. 2), which permit the evaluation of the derivatives with respect to z:

Continuity

$$\frac{\partial v_z'}{\partial z'} \int_0^{2\pi} \rho' \, d\theta' + 2\pi v_z' \frac{\partial \rho'}{\partial z'} = \mathscr{L} f(\gamma) \int_0^{2\pi} \omega' \, d\theta' \tag{5}$$

Momentum in z-direction

$$v_z' \frac{\partial v_z'}{\partial z'} \int_0^{2\pi} \rho' \, d\theta' + \frac{1}{\gamma}\left(\frac{\partial \rho'}{\partial z'} \int_0^{2\pi} T' \, d\theta' + \frac{\partial T'}{\partial z'} \int_0^{2\pi} \rho' \, d\theta'\right) = - \mathscr{L} \Delta v' f(\gamma) \int_0^{2\pi} \omega' \, d\theta' \tag{6}$$

Energy

$$v_z' \frac{\partial T'}{\partial z'} \int_0^{2\pi} \rho' \, d\theta' + (\gamma - 1) \frac{\partial v_z'}{\partial z'} \int_0^{2\pi} P_c' \, d\theta' = \frac{8\pi\gamma}{3} (\gamma - 1) \mathscr{J} f(\gamma) \left(\frac{\partial v_z'}{\partial z'}\right)^2 + \mathscr{L} f(\gamma) \int_0^{2\pi} \omega' \left[(\gamma - T') + \gamma\left(\frac{\gamma - 1}{2}\right)(\Delta v')^2\right] d\theta' \tag{7}$$

Ideal gas

$$2\pi \frac{\partial P_c'}{\partial z'} = \frac{\partial \rho'}{\partial z'} \int_0^{2\pi} T' \, d\theta' + \frac{\partial T'}{\partial z'} \int_0^{2\pi} \rho' \, d\theta' \tag{8}$$

Combustion Models for Burning Rate

In addition to the transport equations, an expression for the instantaneous local burning rate is required. A schematic model for the entire combustion process is illustrated in figure 2. Propellants are assumed to enter the chamber at a varying rate ω_i dependent on the injector pressure drop $P_T - P_c$, which assumes no inertial or capacitance factors in the feed system. (The derivations of expressions for various

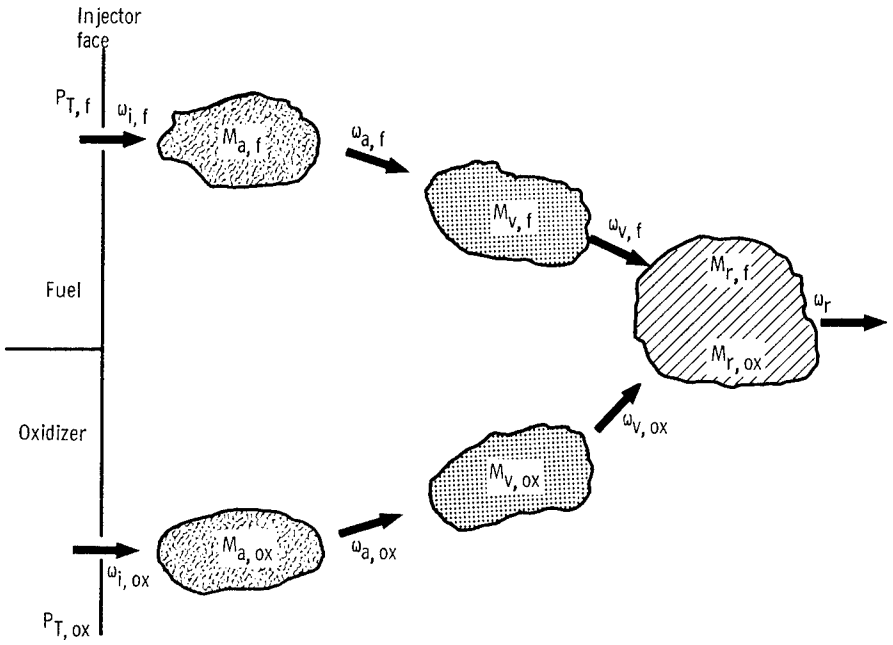

Figure 2. - Schematic model of combustion process.

rates and masses are given in appendix B.) Liquid is atomized at a rate ω_a dependent on the amount of unatomized liquid M_a. Similarly, the propellants vaporize at a rate ω_v depending on the amount atomized but not vaporized M_v and then react chemically at a rate ω_r depending on the amount of each propellant vaporized but unreacted M_r. In figure 2 the arrows represent propellants changing from one state to another, and the crosshatched areas indicate propellants in a given state. The steps between propellant vaporization and reaction must include mixing, but since there are no known expressions to determine the local instantaneous mixing rate, it was not included in the model.

To determine the relative importance of the various combustion steps in driving a pressure oscillation, several models were used. Each model assumed that one of the mechanisms controlled the local instantaneous combustion rate and that the other mechanisms exerted negligible effect on the overall rate; subsequent mechanisms were considered very fast so that they would follow at the same rate. Preparatory mechanisms were considered fast enough to follow the injection rate and yet be insensitive to local fluctuations. With each model an adiabatic pressure disturbance was applied to the system, and its growth, or decay, was observed. This disturbance was given by

$$P_c' = 1 + \frac{P_p}{2} \sin \theta' \tag{9a}$$

$$T' = \left(1 + \frac{P_p}{2} \sin \theta'\right)^{(\gamma-1)/\gamma} \tag{9b}$$

$$\rho' = \left(1 + \frac{P_p}{2} \sin \theta'\right)^{1/\gamma} \tag{9c}$$

Chemical Reaction Model

For this model it was assumed that only the chemical reaction rate varied during instability. The burning rate expression was then

$$\omega' = \omega'_r = M'_{r,ox} M'_{r,f} \exp\left[\frac{E}{\mathcal{R} T_o}\left(1 - \frac{1}{T'}\right)\right] \tag{10}$$

$$M'_{r,ox} = 1 + \frac{2\pi \mathcal{S} f(\gamma)}{\mathcal{C}_{o,ox}} \int_0^{t'} (\omega'_{v,ox} - \omega'_r)\, dt'$$

since

$$\omega'_v = 1 \tag{11a}$$

$$M'_{r,ox} = 1 + \frac{2\pi \mathcal{S} f(\gamma)}{\mathcal{C}_{o,ox}} \int_0^{t'} (1 - \omega')dt' \tag{11b}$$

$$M'_{r,f} = 1 + \frac{2\pi \mathcal{S} f(\gamma)}{\mathcal{C}_{o,f}} \int_0^{t'} (1 - \omega')dt' \tag{11c}$$

Vaporization Model

For this model it was assumed that the vaporization rates for oxidizer and fuel were equal and were the slowest compared to those of the other rates. It was also assumed that the atomization and chemical reaction mechanisms were very rapid so that they followed the injection and vaporization rates, respectively, or

$$\omega'_a \equiv \omega'_i$$

and

$$\omega'_r \equiv \omega'_v$$

The burning rate expression then becomes

$$\omega' = \omega'_{v,f} = \omega'_{v,ox} = (M'_v)^{1/2}(\rho')^{1/2}\left[1 + \left(\frac{v_\theta}{\Delta v}\right)^2\right]^{1/4} \tag{12}$$

$$M'_{v,f} = M'_{v,ox} = 1 + \frac{\omega_{i,o}}{M_{v,o}} t_w \int_0^{t'} (\omega'_{a,ox} - \omega'_v)dt' \tag{13a}$$

$$= 1 + \frac{\omega_{i,o}}{M_{v,o}} t_w \int_0^{t'} (\omega'_i - \omega')dt' \tag{13b}$$

$$\omega'_{i,ox} = \omega'_{i,f} = \sqrt{1 - \frac{P'_c - 1}{\Delta P'}} \tag{14}$$

Atomization Model

It was assumed that the atomization rates for oxidizer and fuel were equal and were the slowest for this model and that the vaporization and chemical reaction followed them, or

$$\omega'_v \equiv \omega'_r \equiv \omega'_a$$

The burning rate was then obtained from

$$\omega' = \omega'_{a,ox} = \omega'_{a,f} = M'_a(\rho')^{5/12}\left[1 + \left(\frac{v'_\theta}{\Delta v'}\right)^2\right]^{0.625} \tag{15}$$

$$M'_{a,ox} = M'_{a,f} = 1 + \frac{\omega_{i,o}}{M_{a,o}} t_w \int_0^{t'} (\omega'_i - \omega'_a)dt' \tag{16}$$

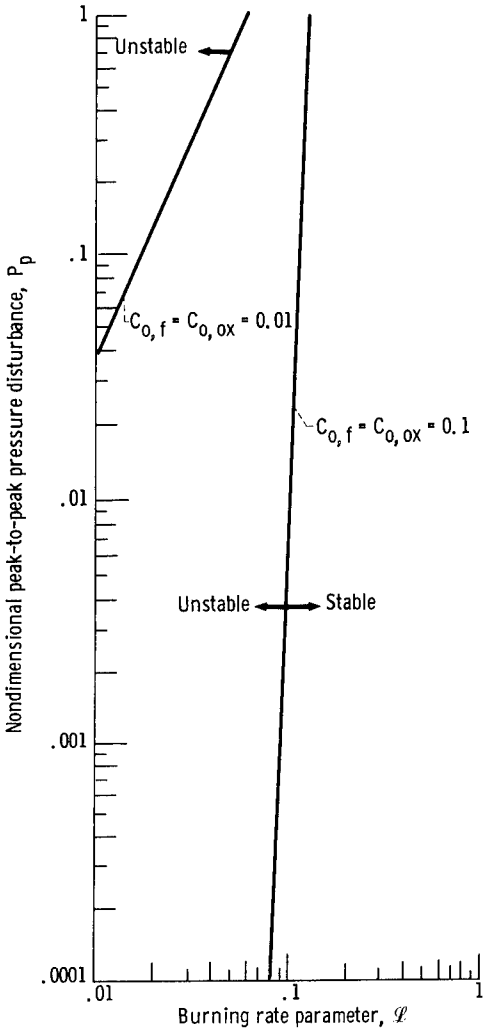

Figure 3. - Instability boundaries for chemical reaction model with finite concentrations.

$$\omega'_{i,ox} = \omega'_{i,f} = \sqrt{1 - \frac{P'_c - 1}{\Delta P'}} \tag{17}$$

THEORETICAL RESULTS

The results of the numerical calculations were pressure, particle velocity, density, temperature, burning rate, and concentration of mass at each of 20 positions in the annulus as functions of time. Typical plots of pressure and velocity can be found in reference 2. From these types of curves it was possible to determine the amplitude of the minimum disturbance that would increase with time. This value of the minimum disturbance was used to determine the boundaries between stable and unstable combustion.

All calculations presented herein were for the following conditions of $\mathcal{J}$, v_z', $\Delta P'$, $\Delta v'$, and γ in equations (1) to (17):

Viscous-dissipation parameter, $\mathcal{J}$	0.3×10^{-7}
Nondimensional axial gas velocity, v_z'	0.05
Nondimensional steady-state pressure drop across injector, $\Delta P'$	0.2
Nondimensional axial velocity difference, $\Delta v'$	0.01
Specific-heat ratio, γ	1.2

The influence of these parameters on the calculated results can be found in reference 2.

Chemical Reaction Model

Stability limits for the chemical reaction-rate model are shown in figure 3 for a limited supply. With an unlimited supply all disturbances that were tested excited instability under all operating conditions ($\mathcal{L}$ values) because of the extreme sensitivity of the exponential function of the chemical reaction equation to a disturbance. However, when a realistic value for the concentration of unburned propellant is used (0.1 or 0.01 mass fraction), the stability limits occur at very low burning rate parameters ($\mathcal{L}$ = 0.1 or less). As discussed in reference 2, these low burning rate parameters occur only for specialized small-scale research combustors.

Vaporization Model

Stability boundaries for the vaporization model are shown in figure 4. The boundary for infinite supply ($M_{v,o}/\omega_{i,o}t_w = \alpha$) is the same as that shown in reference 2 for a value of $\Delta v'$ of 0.01. As the quantity of unvaporized material decreases, the stability limits are increased. (A larger amplitude of disturbance P_p is required to excite instability.) Since $M_{v,o}/\omega_{i,o}t_w$ is equivalent to the ratio of the time to burn an average particle of propellant to the wave time, it is seen that, when the burning time is much less than the wave time, for example, $M_{v,o}/\omega_{i,o}t_w = 1/2\pi$, an extremely large disturbance is required to excite the instability.

The explanation for the increased stability with lower values of $M_{v,o}/\omega_{i,o}t_w$ can be obtained from figure 5, which shows the time histories for the local burning rate, the unvaporized mass, and the pressure at two values of $M_{v,o}/\omega_{i,o}t_w$. With large values of $M_{v,o}/\omega_{i,o}t_w$ the unvaporized mass remains constant during the disturbance, while for low values of $M_{v,o}/\omega_{i,o}t_w$ the unvaporized mass decreases as the pressure and

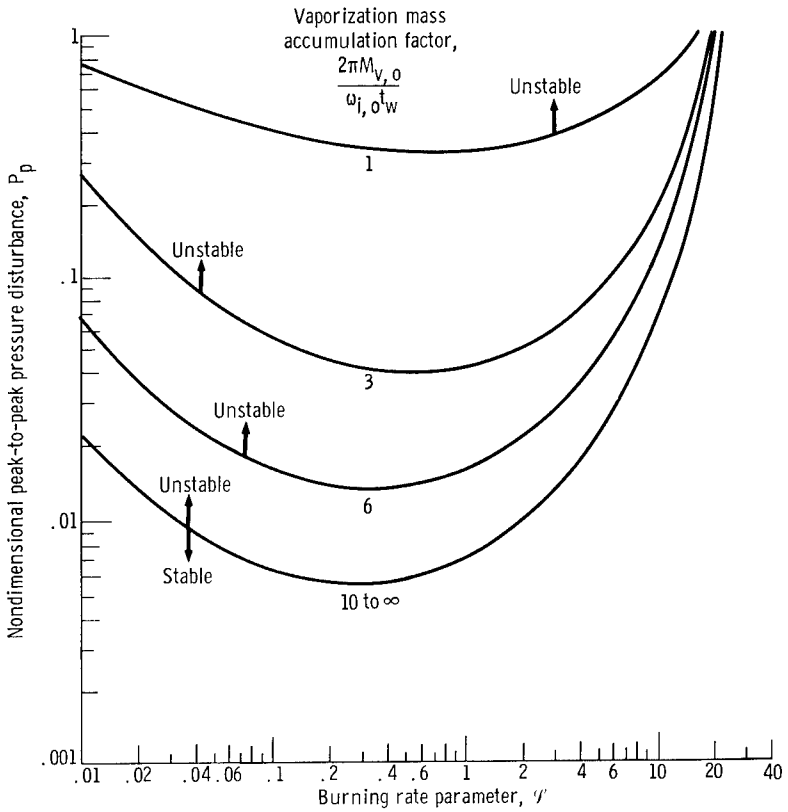

Figure 4. - Instability boundaries for vaporization model.

burning rate increase. Since the burning rate as given by equation (12) is proportional to the square root of the unvaporized mass, the burning rate is reduced by the unvaporized-mass term during the first 1/4 cycle of the disturbance. This reduction results in less energy being added to the wave; hence, the disturbance decays.

Atomization Model

Stability boundaries for the atomization model are shown in figure 6. Stability lines are again shown for various values of $M_{a,o}/\omega_{i,o} t_w$. When the stability boundaries for the vaporization model (fig. 4) are compared with those for the atomization model (fig. 6), it is seen that in some regions the vaporization process is more sensitive to a disturbance and that in other regions the atomization process has the greater sensitivity. Therefore, both processes must be considered important in controlling combustion instability.

Time histories of unatomized liquid, burning rate, and pressure are shown for the atomization model in figure 7. The histories are similar to those in figure 6 for the vaporization model; that is, for large values of $M_{a,o}/\omega_{i,o} t_w$ the system is unstable,

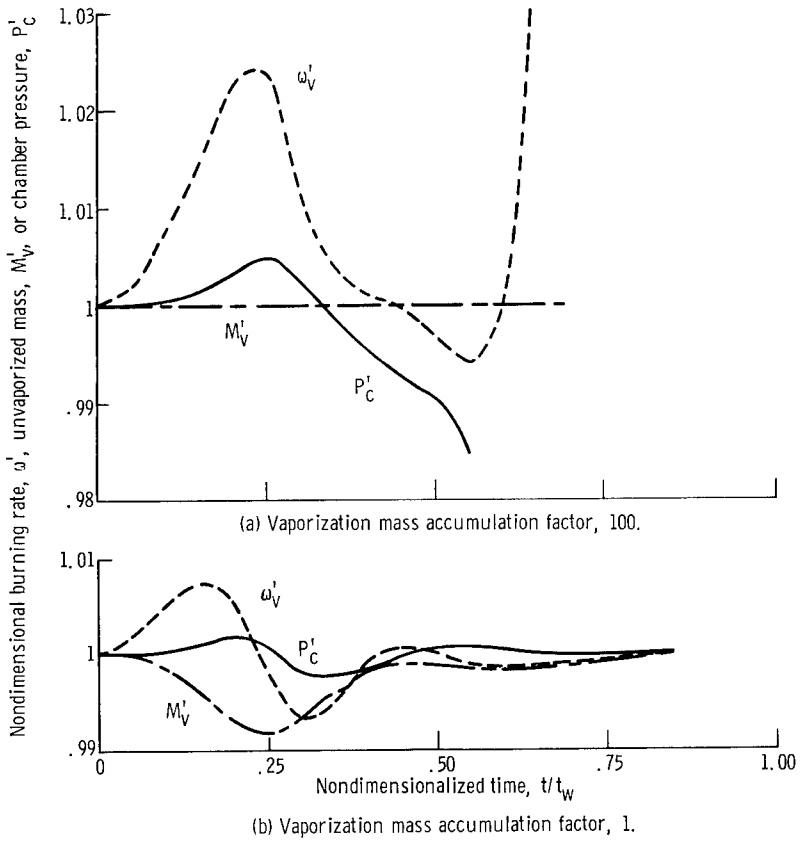

Figure 5. - Time history of disturbance for vaporization model. Burning-rate parameter, 1; nondimensional peak-to-peak pressure disturbance, 0.01.

and the unatomized liquid remains constant. For small values of $M_{a,o}/\omega_{i,o}t_w$ the system is stable, and the unatomized liquid decreases as the burning rate and pressure are increased. This decrease in unatomized liquid reduces the burning rate, which results in insufficient energy to drive the disturbance.

Vortex Flow Model

Recent studies (ref. 3) have shown that with viscous forces a transverse pressure oscillation can generate a vortex within the combustor. Therefore to determine the significance of such a flow pattern, additional calculations were performed to determine the influence of a vortex on stability. These calculations were performed by using the vaporization model with a constant vortex velocity v_{vr} added to the calculated values of gas velocity in the tangential direction, v_θ. Results of these calculations are illustrated in figure 8. The stability limits are dramatically changed by a small vortex velocity. For a given vortex velocity the system has the same stability at low burning rate parameters that it had for the vaporization model. At some critical burning rate param-

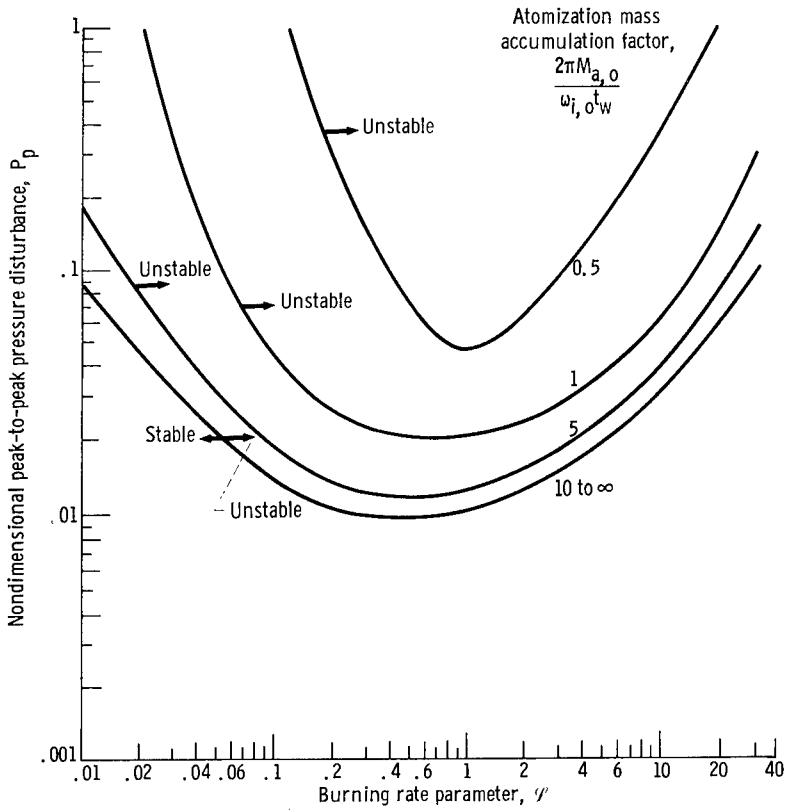

Figure 6. - Instability boundaries for atomization model.

eters, dependent on the vortex velocity, the vortex model shows that almost any disturbance will grow. Larger critical burning rate parameters are required for smaller vortex velocities. The effectiveness of baffles can be partially explained by the vortex model results. The vortex velocity can be eliminated by using baffles, and the stability of the vaporization model boundaries can thus be increased.

The vortex model can also explain the results reported for the investigation of reference 4, in which a tangential gas flow was used to excite instability. The quantity of tangential gas flow required to induce instability was dependent on the operating conditions of the combustor.

EXPERIMENTAL RESULTS

To test the validity of the theoretical results, an experimental program was also conducted. Since the calculations were only performed for an annular segment of a combustor, an annular or torus combustor was used in the experimental program (fig. 9, p. 15). The torus had an 8-foot diameter and 10 injectors with nozzles equally spaced around the chamber. Four different types of injectors were used to change the operating

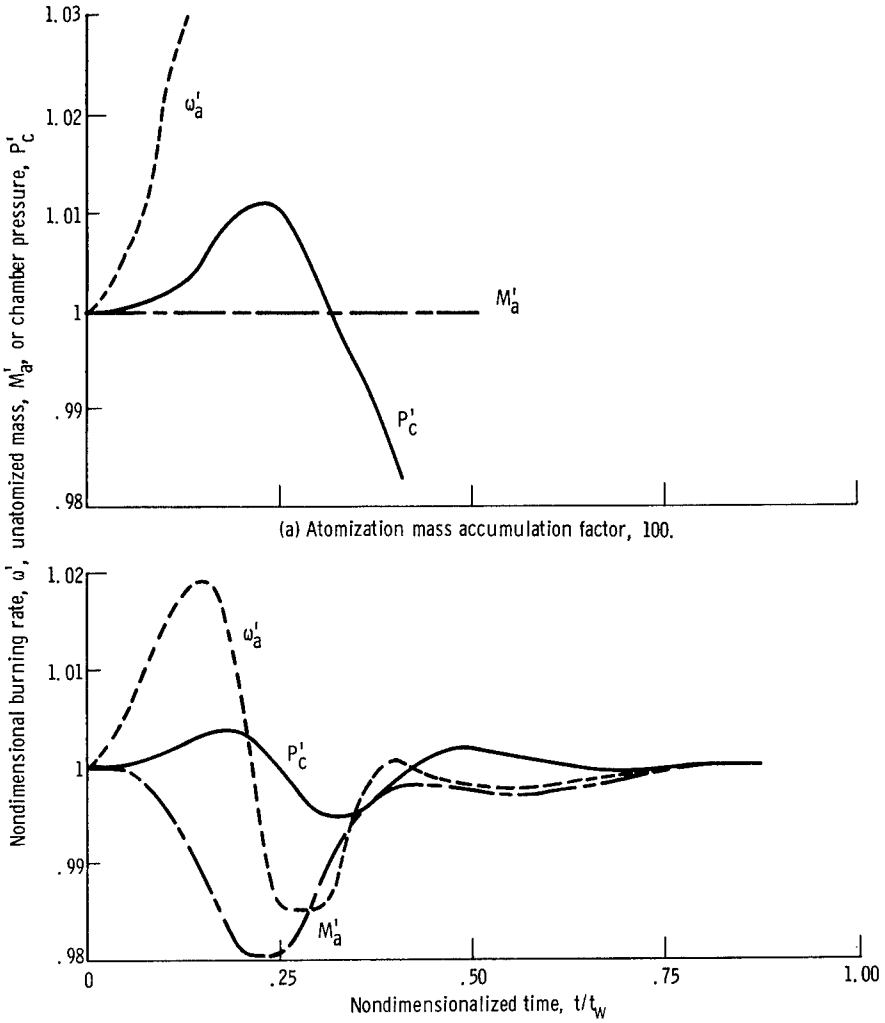

Figure 7. - Time history for atomization model. Burning-rate parameter, 1; nondimensional peak-to-peak pressure disturbance, 0.02.

conditions. The injectors (shown in fig. 9) were (1) an unlike-triplet injector with two hydrogen streams impinging on one liquid-oxygen jet, (2) an impinging-jet injector with two liquid-oxygen jets impinging on each other and four parallel jets of hydrogen, (3) a coarse parallel-jet injector with one jet of liquid oxygen and two jets of hydrogen, (4) a fine parallel-jet injector with four jets of liquid oxygen and four of hydrogen. Two-inch-diameter windows were placed in the combustor so that the combustion process could be observed and the steady combustion characteristics established.

The torus combustor was operated over the following range of conditions:

Steady-state chamber pressure, $P_{c,o}$, lb/sq in. abs	40 to 120
Oxidizer-flow rate, lb/sec	0.95 to 3.5
Fuel-flow rate, lb/sec	0.15 to 0.45

Total flow rate, lb/sec	1.2 to 4.0
Oxidizer-fuel weight ratio	2.0 to 8.0
Oxidizer injection velocity, $v_{i,ox}$, ft/sec	15 to 55
Hydrogen injection velocity, $v_{H_2,i}$, ft/sec	300 to 600
Oxidizer pressure drop, $\Delta P'_{ox}$	0.2 to 0.8
Hydrogen temperature, ^{o}F	32 to 80
Liquid-oxygen temperature, ^{o}F	-320

To excite instability a tangential blast tube 10 feet long with a 2-inch inside diameter was added to the combustor. A burst disk that ruptured at 1000 pounds per square inch was placed at the combustor end of the blast tube. The tube was loaded with 75 grams of ammonium perchlorate containing 25 percent by weight polybutadiene acrylic acid, which was ignited during the run and which provided sufficient gas to burst the diaphragm and

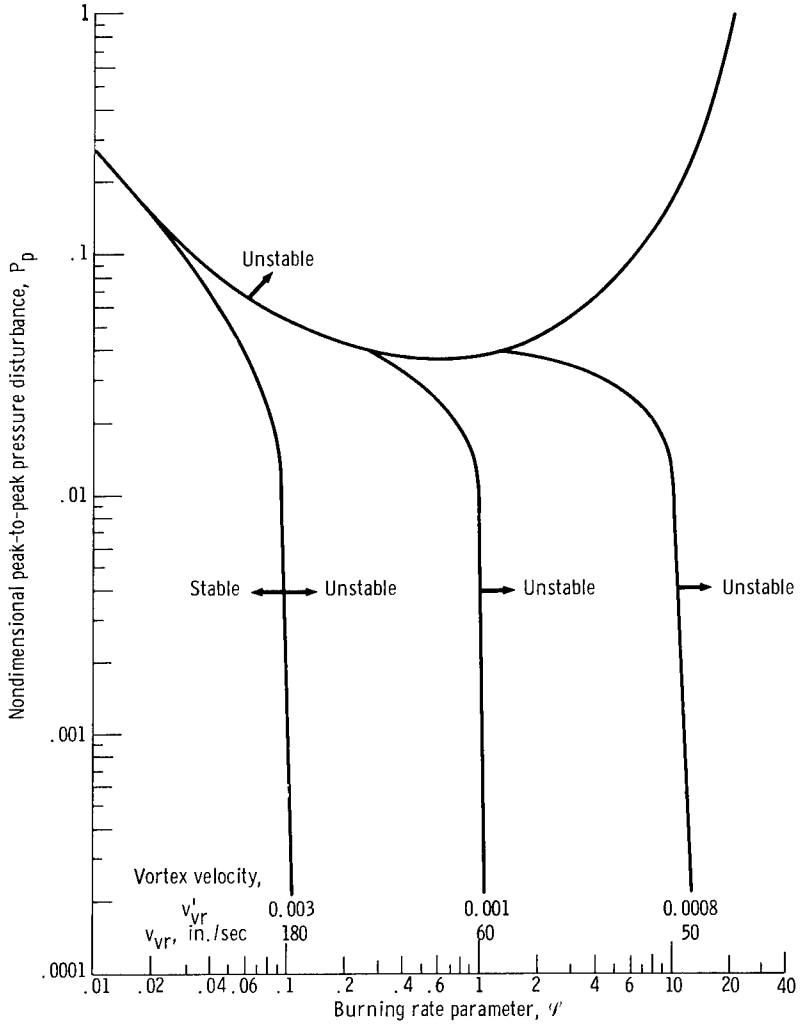

Figure 8. - Instability boundaries for vaporization model with vortex flow.

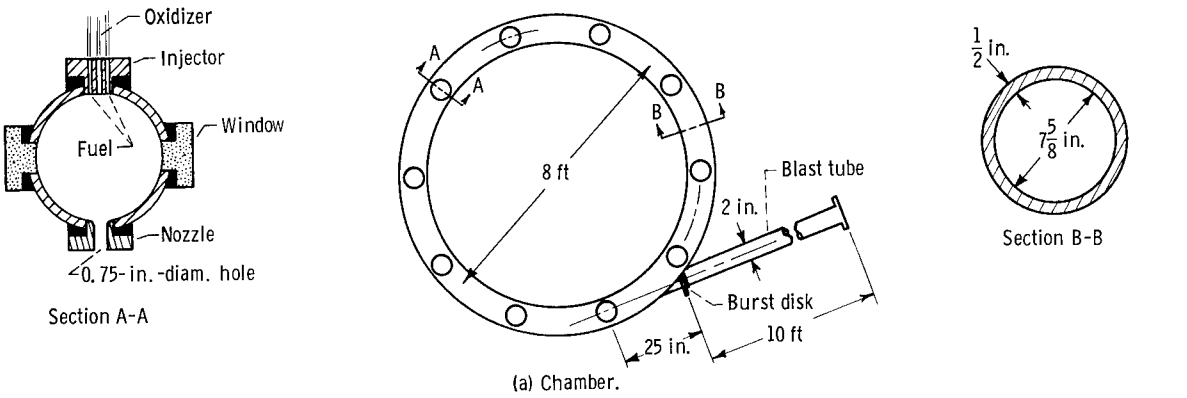

(a) Chamber.

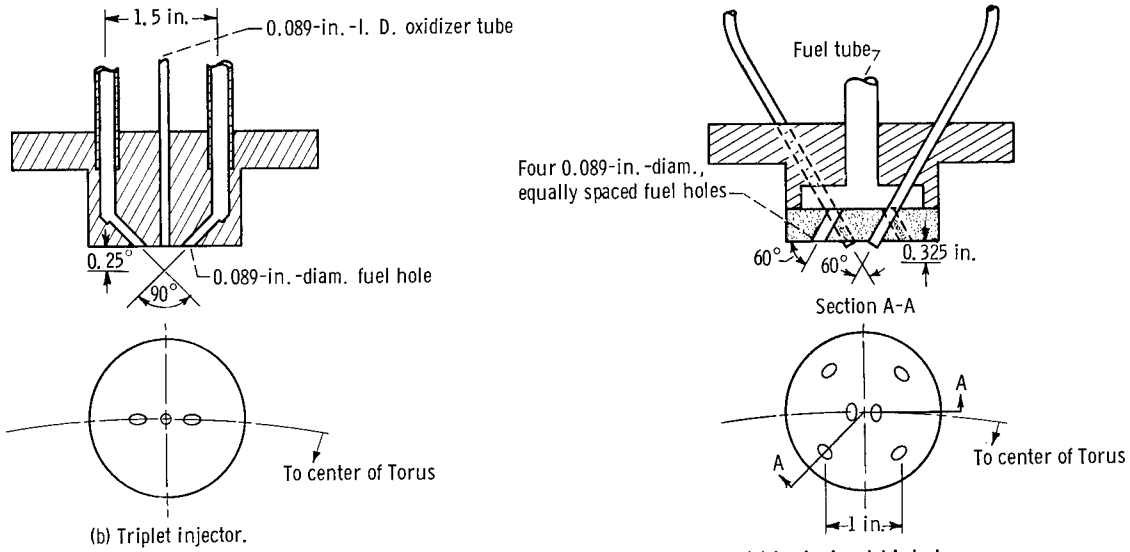

(b) Triplet injector.

(c) Impinging-jet injector.

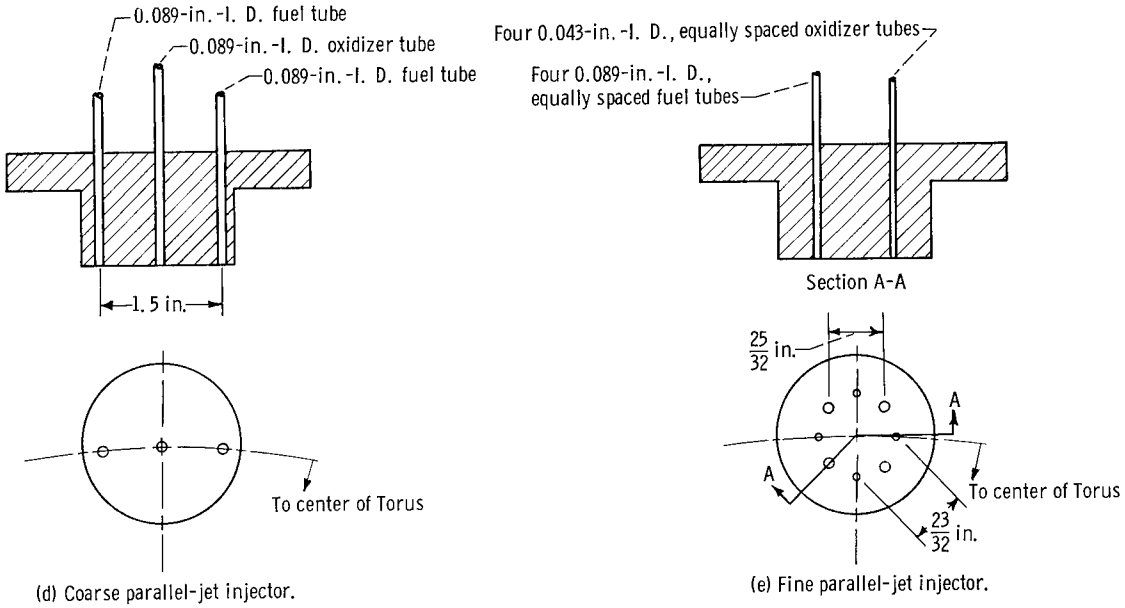

(d) Coarse parallel-jet injector.

(e) Fine parallel-jet injector.

Figure 9. - Torus combustor.

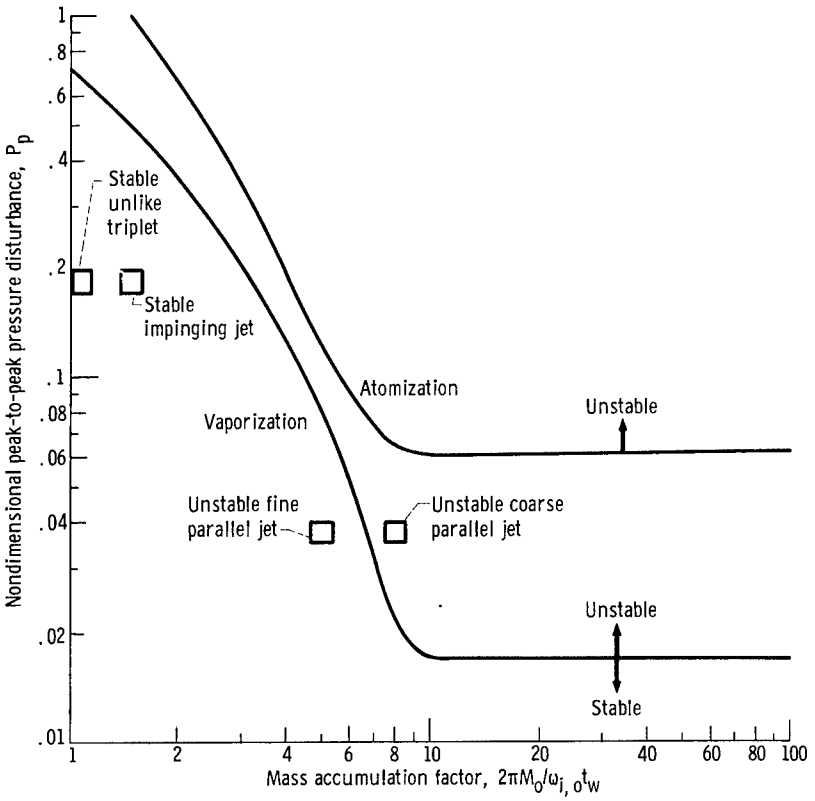

Figure 10. - Experimental and theoretical stability boundaries for torus combustor. Burning-rate parameter, 0.015.

produce a peak-to-peak pressure oscillation of 20 percent of the chamber pressure in the torus combustor.

The experimental results are shown in figure 10, where the disturbance amplitude is plotted against the mass accumulation factor $2\pi M_o/\omega_{i,o}t_w$. For the unlike-triplet and impinging-jet injectors the 20-percent disturbance always damped. The instability of all runs with the two parallel-jet injectors indicated that the combustion noise produced disturbances large enough to excite instability. The noise level was assumed to be the same as that observed for the triplet and impinging-jet injectors during steady-state combustion (4 percent of chamber pressure), although larger disturbances were present during ignition and while flows were adjusting to their average rate. The instability was always initiated sometime after ignition but before average flow rates were achieved.

The curves in figure 10 are cross plots of data presented in figures 4 and 6 for a burning rate parameter of 0.015. This value of $\mathscr{L}$ is for the torus with a radius $\mathscr{R}$ of 48 inches, an average burning rate per total length of combustor m of 0.131, and a combustor contraction ratio $\mathscr{A}$ of 409 (obtained by dividing the volume of the combustor by the product of the nozzle area and the distance from the injector to the nozzle). The theoretical curves show that the vaporization model has a slightly lower instability limit than the atomization model for the operating conditions of the torus combustor. The ex-

perimental value of the mass accumulation factor was obtained by calculating the amount of vaporized propellant as a function of length (ref. 5). These calculations agreed with the observation at the window that all of the propellant was vaporized for the impinging-jet and triplet injectors, while only a small fraction was vaporized with the parallel-jet injectors. Thus the parallel-jet-type injectors provided sufficient liquid in the combustor to significantly reduce the calculated disturbance amplitude required to excite instability.

The experimental and calculated results shown in figure 10 indicate that good agreement exists between theory and experiment. Theory indicates that a disturbance greater than 40 percent is required to excite instability with the impinging-jet and triplet injectors, and experiments showed that a 20-percent disturbance would decay. Similarly, the parallel-jet-type injectors, which were always unstable, should require only a 2- to 6-percent disturbance to excite instability. Operating conditions of the torus combustor did not completely agree with the conditions used in the calculations. However, these would not significantly change the calculated curves because the calculations are quite insensitive to $\mathcal{J}$, v_z', $\Delta P'$, and γ. The minimum disturbance is very sensitive to $\Delta v'$; however, the value of 0.01 for $\Delta v'$ is very reasonable in that it represents the turbulence level available as a driving source when gas and liquid velocities are very low.

High-speed motion pictures taken of the sprays during instability indicated that the sprays were undergoing breakup due to crossflow at the high-pressure portion of the oscillations. It was impossible to determine the rate of breakup or vaporization, however, because the liquid-oxygen sprays are not clearly outlined in the pictures; therefore, the volume of liquid could not be measured accurately enough to obtain slopes and hence atomization or vaporization rates. The amount of liquid in the combustor varied during the cycle as predicted by the theory.

SUMMARY OF RESULTS

Theoretical calculations have shown that the physical processes of vaporization and atomization probably are the controlling parts of the combustion process in determining combustion instability. Chemical reaction is not likely to be important for most rocket combustors because there is insufficient mass or energy available in gaseous form to sustain an oscillation even though the reaction rate is very sensitive to pressure, velocity, or temperature variations.

Theory also indicates that the stability of a combustor is very dependent on the mass of liquid in the combustor and the existence of any vortex velocity, as well as the velocity difference and the burning rate parameter (ref. 2).

Limited experimental studies with a combustor similar to the one used in the theory have confirmed the stability regions. Experiments also confirm qualitatively the variations that occur during an oscillation.

Lewis Research Center,
National Aeronautics and Space Administration,
Cleveland, Ohio, February 9, 1965.

APPENDIX A

SYMBOLS

A_c	cross-sectional area of combustor, sq in.
A_d	average surface area of drops, sq in.
A_i	injection hole area, sq in.
A_t	nozzle-throat area, sq in.
$\mathcal{A}$	combustor contraction ratio, A_c/A_t, dimensionless
a	average speed of sound in gases, in./sec
C_D	coefficient of discharge of injector, dimensionless
$\mathcal{C}_o$	average steady-state mass fraction of unburned gases, dimensionless
c*	characteristic exhaust velocity, ft/sec
D	molecular diffusion coefficient, sq in./sec
E	activation energy, in. lb/lb mole
$f(\gamma)$	function of gamma, $\sqrt{\left(\frac{2}{\gamma+1}\right)^{\gamma+1/\gamma-1}}$
g	acceleration due to gravity, 386.09 in./sec^2
$\mathcal{J}$	viscous-dissipation parameter, $\mu_o c^*/RP_{c,o}g$
k	preexponential constant in Arrhenius equation, cu in./(lb mole)(sec)
$\mathcal{L}$	burning-rate parameter, $Rm/\mathcal{A}$
M	mass concentration, lb/cu in.
M_a	mass concentration of unatomized propellant, lb/cu in.
M_r	mass concentration of unreacted propellant, lb/cu in.
M_v	mass concentration of unvaporized propellant, lb/cu in.
m	average burning rate of propellant per length of combustor, fraction/in.
m_ℓ	molecular weight of propellant, lb mass/lb mole
N_d	number of liquid drops per unit volume in combustor, 1/cu in.
P_c	chamber pressure, lb/sq in.
$P_{c,o}$	steady-state chamber pressure
$P_{c,max}$	maximum chamber pressure
$P_{c,min}$	minimum chamber pressure
P_p	nondimensional peak-to-peak pressure disturbance, $\frac{P_{c,max} - P_{c,min}}{P_{c,o}}$

P_T tank pressure, lb/sq in.

P_v vapor pressure of liquid, lb/sq in.

$\Delta P'$ nondimensional steady-state pressure drop across injector, $\frac{P_T - P_{c,o}}{P_{c,o}}$

R radius of combustor, in.

$\mathscr{R}$ universal gas constant, 18 510 (in.)(lb)/(^oR)(lb mole)

Re Reynolds number, dimensionless

r_d average drop radius, in.

r_j average jet radius, in.

Sc Schmidt number, dimensionless

T temperature, ^oR

t time, sec

t_B breakup time of liquid, sec

t_w average wave time, $2\pi R/a$, sec

t' nondimensional time, t/t_w

U velocity difference between liquid and gas, in./sec

v gas velocity, in./sec

Δv steady-state average axial velocity difference between liquid and gas, in./sec

v' nondimensional gas velocity, v/a

$\Delta v'$ nondimensional axial velocity difference, $\Delta v/a$

v_{vr} steady-state average vortex velocity, in./sec

v'_{vr} nondimensional vortex velocity, v_{vr}/a

v_z axial gas velocity, in./sec

v_θ tangential gas velocity, in./sec

We Weber number, dimensionless

z axial coordinate

z' nondimensional axial coordinate, z/R

α correction factor for mass transfer, dimensionless

γ specific-heat ratio, dimensionless

θ angular coordinate

μ gas viscosity, lb/(in.)(sec)

ρ gas density, lb/cu in.

ω burning rate, lb/(sec)(cu in.)

ω_a atomization rate, lb/(sec)(cu in.)

ω_i injection rate, lb/(sec)(cu in.)

ω_r chemical reaction rate, lb/(sec)(cu in.)

ω_v vaporization rate, lb/(sec)(cu in.)

Subscripts:

f fuel

ℓ liquid

o steady-state conditions

ox oxidizer

Superscript:

' nondimensionalized parameter, equal to parameter divided by steady-state parameter, i.e., $T' = T/T_o$ (except for velocities, which are divided by speed of sound, and time, which is divided by wave time)

APPENDIX B

EQUATIONS FOR RATES AND MASSES

Injection Rate

The local instantaneous injection rate is given by

$$\omega_i = C_D A_i \sqrt{(P_T - P_c) 2 \rho_\ell g} \tag{B1}$$

The steady-state injection rate is

$$\omega_{i,o} = C_D A_i \sqrt{(P_T - P_{c,o}) 2 \rho_\ell g} \tag{B2}$$

$$\omega_i' = \frac{\omega_i}{\omega_{i,o}} = \sqrt{\frac{P_T - P_c}{P_T - P_{c,o}}}$$

$$= \sqrt{1 - \frac{P_c' - 1}{\Delta P'}} \tag{B3}$$

Atomization Rate

The time to atomize a jet or drop of liquid in a cross current for values of $We/Re^{1/2}$ much larger than 1 is (ref. 6)

$$t_B = 6.43 \left(\frac{\rho_\ell}{\rho}\right)^{2/3} \left(\frac{\mu}{\mu_\ell}\right)^{1/3} \frac{r_j}{U} \frac{Re^{3/4}}{(2We)^{1/2}} \tag{B4}$$

where $Re = r_j(U\rho/\mu)$ and $We = r_j(\rho U^2/\sigma)$. If the instantaneous atomization is the same as the average for complete breakup, the atomization rate is

$$\omega_a = \frac{M_a}{t_B}$$

and

$$\omega_{a,o} = \frac{M_{a,o}}{t_{B,o}}$$

then

$$\omega_a' = \frac{\omega_a}{\omega_{a,o}} = M_a'(\rho')^{5/12}\left(\frac{U}{U_o}\right)^{1.25}$$

$$= M_a'(\rho')^{5/12}\left[\frac{v_\theta^2 + (\Delta v)^2}{(\Delta v)^2}\right]^{0.625}$$

$$= M_a'(\rho')^{5/12}\left[1 + \left(\frac{v_\theta'}{\Delta v'}\right)^2\right]^{0.625} \tag{B5}$$

Vaporization Rate

The rates of vaporization for large Reynolds numbers as given in reference 1 are as follows:

$$\omega_v = \frac{N_d D \mathscr{m}_\ell A_d \alpha P_v}{\mathscr{R}\, T 2 r_d}\, 0.6\, Sc^{1/3}\left[2r_d(v - v_{\ell,o})\right]^{1/2}\left(\frac{\rho}{\mu}\right)^{1/2} \tag{B6}$$

$$\omega_{v,o} = \frac{N_d D \mathscr{m}_\ell A_{d,o} \alpha P_v}{\mathscr{R}\, T 2 r_{d,o}}\, 0.6\, Sc^{1/3}\left[2r_{d,o}(v - v_{\ell,o})\right]^{1/2}\left(\frac{\rho}{\mu}\right)^{1/2} \tag{B7}$$

$$\omega_v' = \frac{\omega_v}{\omega_{v,o}} = \frac{A_d}{A_{d,o}}\left(\frac{r_{d,o}}{r_d}\right)^{1/2}\left(\frac{\rho}{\rho_o}\right)^{1/2}\left(\frac{v - v_{\ell,o}}{v_o - v_{\ell,o}}\right)^{1/2} \tag{B8}$$

$$\omega_v' = \left(\frac{r_d}{r_{d,o}}\right)^{3/2}\left(\frac{\rho}{\rho_o}\right)^{1/2}\left(\frac{v_\theta^2 + \Delta v^2}{\Delta v^2}\right)^{1/4} \tag{B9}$$

$$\omega_v' = (M_v')^{1/2}(\rho')^{1/2}\left[1 + \left(\frac{v_\theta'}{\Delta v'}\right)^2\right]^{1/4} \tag{B10}$$

Chemical Reaction Rate

The chemical reaction rate is given by a second-order rate expression in which an Arrhenius rate constant is assumed:

$$\frac{\omega_r}{m_{ox,f}} = \frac{M_{r,ox}}{m_{ox}}\frac{M_{r,f}}{m_f} k \exp\left(\frac{-E}{\mathcal{R}T}\right) \tag{B11}$$

$$\frac{\omega_{r,o}}{m_{ox,f}} = \frac{M_{r,ox,o}}{m_{ox}}\frac{M_{r,f,o}}{m_f} k \exp\left(\frac{-E}{\mathcal{R}T_o}\right) \tag{B12}$$

$$\omega_r' = \frac{\omega_r}{\omega_{r,o}} = M_{r,ox}'M_{r,f}' \exp\left[\frac{E}{\mathcal{R}T_o}\left(1 - \frac{1}{T'}\right)\right] \tag{B13}$$

Mass of Unatomized Propellant

The mass of unatomized propellant is determined by a mass balance:

$$M_a = M_{a,o} + \int_0^t (\omega_i - \omega_a)dt \tag{B14}$$

$$M_a' = \frac{M_a}{M_{a,o}} = 1 + \frac{\omega_{i,o}}{M_{a,o}}\int_0^t \left(\frac{\omega_i}{\omega_{i,o}} - \frac{\omega_a}{\omega_{i,o}}\right) t_w \, dt' \tag{B15}$$

Assuming that all the propellant is consumed in the combustor gives

$$\omega_{v,o} = \omega_{i,o} = \omega_{a,o}$$

$$M_a' = 1 + \frac{\omega_{i,o}}{M_{a,o}} t_w \int_0^{t'} (\omega_i' - \omega_a')dt' \tag{B16}$$

Mass of Unvaporized Propellant

The mass of unvaporized propellant is also determined by a mass balance:

$$M_v = M_{v,o} + \int_0^t (\omega_a - \omega_v)dt \tag{B17}$$

$$M_v' = \frac{M_v}{M_{v,o}} = 1 + \frac{\omega_{i,o}}{M_{v,o}} \int_0^{t'} \left(\frac{\omega_a}{\omega_{i,o}} - \frac{\omega_v}{\omega_{i,o}} \right) t_w \, dt' \tag{B18}$$

since

$$\omega_{v,o} = \omega_{i,o} = \omega_{a,o} \tag{B19}$$

$$M_v' = 1 + \frac{\omega_{i,o}}{M_{v,o}} t_w \int_0^{t'} (\omega_a' - \omega_v')dt' \tag{B20}$$

Mass of Unreacted Propellant

The amount of unreacted propellant is also determined by a mass balance:

$$M_r = M_{r,o} + \int_0^t (\omega_v - \omega_r)dt \tag{B21}$$

where

$$M_{r,o} = \mathscr{C}_o \rho_o \tag{B22}$$

$$M_r' = 1 + \frac{\omega_{i,o}}{\mathscr{C}_o \rho_o} \int_0^{t'} \left(\frac{\omega_v}{\omega_{i,o}} - \frac{\omega_r}{\omega_{i,o}} \right) t_w \, dt' \tag{B23}$$

since

$$\frac{\omega_{i,o} t_w}{\rho_o} = \frac{\omega_{i,o} 2\pi R}{\rho_o a} = 2\pi \mathscr{S} f(\gamma)$$

(See eqs. (A29) and (A31) of ref. 2.)

$$M_r' = 1 + \frac{2\pi \mathscr{S} f(\gamma)}{\mathscr{C}_o} \int_0^{t'} (\omega_v' - \omega_r') dt' \tag{B24}$$

REFERENCES

1. Priem, Richard J.: Theoretical and Experimental Models for Unstable Rocket Combustor. Ninth Symposium (International) on Combustion, Academic Press, 1963, pp. 982-992.

2. Priem, Richard J.; and Guentert, Donald C.: Combustion Instability Limits Determined by a Nonlinear Theory and a One-Dimensional Model. NASA TN D-1409, 1962.

3. Swithenbank, J.; and Sotter, G.: Vortex Generation in Solid Propellant Rockets. AIAA J., vol. 2, no. 7, July 1964, pp. 1297-1302.

4. Heidmann, M. F.: Oxygen-Jet Behavior During Combustion Instability in a Two-Dimensional Combustor. NASA TP 2-63, 1963.

5. Priem, Richard J.; and Heidmann, Marcus F.: Propellant Vaporization as a Design Criterion for Rocket-Engine Combustion Chambers. NASA TR R-67, 1960.

6. Morrell, Gerald: Rate of Liquid Jet Breakup by a Transverse Shock Wave. NASA TN D-1728, 1963.

"The aeronautical and space activities of the United States shall be conducted so as to contribute . . . to the expansion of human knowledge of phenomena in the atmosphere and space. The Administration shall provide for the widest practicable and appropriate dissemination of information concerning its activities and the results thereof."

—NATIONAL AERONAUTICS AND SPACE ACT OF 1958

NASA SCIENTIFIC AND TECHNICAL PUBLICATIONS

TECHNICAL REPORTS: Scientific and technical information considered important, complete, and a lasting contribution to existing knowledge.

TECHNICAL NOTES: Information less broad in scope but nevertheless of importance as a contribution to existing knowledge.

TECHNICAL MEMORANDUMS: Information receiving limited distribution because of preliminary data, security classification, or other reasons.

CONTRACTOR REPORTS: Technical information generated in connection with a NASA contract or grant and released under NASA auspices.

TECHNICAL TRANSLATIONS: Information published in a foreign language considered to merit NASA distribution in English.

TECHNICAL REPRINTS: Information derived from NASA activities and initially published in the form of journal articles.

SPECIAL PUBLICATIONS: Information derived from or of value to NASA activities but not necessarily reporting the results of individual NASA-programmed scientific efforts. Publications include conference proceedings, monographs, data compilations, handbooks, sourcebooks, and special bibliographies.

Details on the availability of these publications may be obtained from:

SCIENTIFIC AND TECHNICAL INFORMATION DIVISION

NATIONAL AERONAUTICS AND SPACE ADMINISTRATION

Washington, D.C. 20546